AIMS Biophysics

AIMS Biophysics, 7(1): 54–64.
DOI: 10.3934/biophy.2020005
Received: 03 February 2020
Accepted: 22 March 2020
Published: 25 March 2020

http://www.aimspress.com/journal/biophysics

Research article

Analysis of a normal and aero helmet on an elite cyclist in the dropped position

Pedro Forte[1,2,4,*], Daniel A Marinho[3,4], Tiago M Barbosa[2,4] and Jorge E Morais[1,2,4]

[1] Department of Sports Sciences, Higher Institute of Educational Sciences of the Douro, Penafiel, Portugal
[2] Department of Sports Sciences, Polytechnic Institute of Bragança, Bragança, Portugal
[3] Department of Sports Sciences, University of Beira Interior, Covilhã, Portugal
[4] Research Center in Sports, Health and Human Development, Covilhã, Portugal

*** Correspondence:** Email: pedromiguel.forte@iscedouro.pt; Tel: +351255318550.

Abstract: Cyclists use to wear different helmets and adopt different body positions on the bicycle to minimize resistance. The aim of this study was to compare a standard helmet with the new aero road helmets in a bicycle-cyclist system by CFD on the dropped position. An elite level road cyclist volunteered to this research. The cyclist was scanned on his racing bicycle on the dropped position wearing competition gear and a standard helmet and an aero road helmet. A three-dimensional domain around the cyclist with 7 m of length, 2.5 m of width and 2.5 m of height and meshed with more than 43 million of prismatic and tetrahedral elements. The numerical simulations were conducted at 11.11 m/s. The numerical simulations outputs were viscous, pressure and total drag and coefficient of drag. The standard helmet presented a viscous drag of 10.52 N, a pressure drag of 16.51 N and a total drag of 21.98 N. The aero road helmet presented a pressure drag of 7.40 N, a viscous drag of 12.56 N and a total drag of 19.96 N. Moreover, the aero road helmet presented a lower viscous, pressure and total drag coefficient in comparison to the standard helmet. It is possible to conclude that an aero road helmet imposes less drag in comparison to a standard helmet.

Keywords: cycling; helmets; drag; dropped position

1. Introduction

Cycling has been considered as one of the most popular sports around the world. The major

concern about cyclist's performance is to reach their averaged maximal speed as soon as possible and maintain it over a race. According to Newton's second law (equation 1), acceleration is given by the ration between force and mass (equation 2). Knowing that, cyclists propulsion may overcome the resistance (equation 3) [1].

$$F = m.a \tag{1}$$

Where, F is the force, m the mass and a is the acceleration.

$$a = \frac{F}{m} \tag{2}$$

$$a = \frac{(F_{prop} + F_{res})}{m} \tag{3}$$

Where, F_{prop} are the propulsive forces and F_{res} the resistive forces in negative direction of the motion.

Cyclists aim to improve performance minimizing the winning time and effort during the race. To maintain the averaged speed, cyclists may deliver energy to the pedals. Among the delivered energy by the cyclist, some is necessary to overcome resistance and other lost by the bicycle-cyclist system.

$$v = \sqrt{\frac{2(\varepsilon_{in} - \varepsilon_{loss})}{m}} \tag{4}$$

Some strategies are adopted to reduce the required energy at a given speed or pace. Cyclists used to wear different helmets and adopt different body positions on the bicycle to minimize resistance [2,3]. Drag is the main resistive force in cycling and contributes about 90% of the resistance [4–6]. Among the different positions (normal, dropped and aero), there is the drooped position [7]. This position aims to reduce frontal surface area and drag in comparison to the normal position [7]. Moreover, it is dependent of anthropometrics, trunk position and bicycle control in the different road curves and slopes; whereas the aero position is mainly used in straight events [8–11].

Drag can be assessed by analytical procedures, coasting deceleration methods, wind tunnel testing and numerical simulations by computer fluid dynamics (CFD) [12]. However, CFD has been used to understand the fluid flow behavior around an object [12,13]. This methodology helps to control confounding factors such as temperature, side winds or assumptions such as drag coefficient. Wind tunnel testing is considered the gold standard method; however, the tests are expensive and demand a considered time consumption [12]. The analytical procedures required a set of assumptions and estimations and coasting technics do not allow to control environmental conditions [12].

Helmets designs aim to improve cyclists performance, reducing the winning time. Upon the different helmets type, a so called: (i) standard and; (ii) aero road helmet. This new aero road helmets are characterized by different tail lengths and reduced air vents, intending to improve efficiency and aerodynamics [3,14,15]. Recently, elite road cyclists have been using these "new" aero road helmets due the impossibility to use time-trial helmets in track races. That might be related with the importance of minimize drag and improve efficiency, as in time-trial helmets [3]. However, it is yet unclear what is the effect of these new type of helmets on a rider's aerodynamics.

To date, this is the first attempt that this new type of helmets is tested in the dropped position.

Moreover, most studies with helmets are made in the aero position or only assess the helmet. Thus, the aim of this study was to compare a standard helmet with the new aero road helmets in a bicycle-cyclist system by CFD. It was hypothesized that the aero road helmet imposes a lower drag in the bicycle/cyclist system.

2. Materials and method

2.1. Subject

An elite level road cyclist, racing regularly at national level events volunteered to this research. The bicycle-cyclist system mass was 62 kg (cyclist: 55.0 kg of body mass and 1.76 m of height). All procedures were in accordance to the Helsinki Declaration regarding human research and a written consent was obtained beforehand.

2.2. Scanning the model

The cyclist was scanned on his racing bicycle on the dropped position wearing competition gear and each of the two helmets. The scans were wearing a standard helmet (Figure 1 at left; Giant, Rev Helmet) and an aero road helmet (Figure 1 at right; Giant, Pursuit Helmet) (Figure 1). The Rev Helmet type pull the incoming air from the front and side channels to back; whereas the Pursuit Helmet aims to produce the wind-cheating effects of time-trial helmets to the road without sacrificing ventilation with only two ventilation channels (front and back).

The scanning process was made with a Sense 3D scanner (3D Systems, Inc., Canada) and saved in the Sense Software (Sense, 3D Systems, Inc., Canada). The scanner precision was 0.0009 m (0.9 mm) at 0.5 m (50 cm) distance. The Sense software allowed to clean, fill holes and solidify the geometry, then the model was exported as stereolithographic file (.stl). The Geomagic studio (3D Systems, USA) was used to edit and post process the geometry in stl format. The models were meshed, smoothed, clean self-intersections, spikes and non-manifold edges on Geomagic studio. CAD models were created from the geometries [13] (Figure 1).

Figure 1. Three-dimensional models of the cyclist on the dropped position with a standard (left) and an aero road helmet (right).

2.3. Boundary conditions

In Ansys Workbench software (Ansys Fluent 16.0, Ansys Inc., Pennsylvania, USA) the models were imported to start the numerical simulations process. The boundary dimensions were created in the geometry module with a three-dimensional domain around the cyclist with 7 m of length, 2.5 m of width and 2.5 m of height (Figure 2). The domain was meshed to represent the fluid flow in the opposite direction to the cyclist with more than 43 million of prismatic and tetrahedral elements and the cell size were near 25.72 μm and (Ansys Mesh, Ansys Inc., Pennsylvania, USA). The cyclist was placed at 2.5 meters of the inlet portion [16].

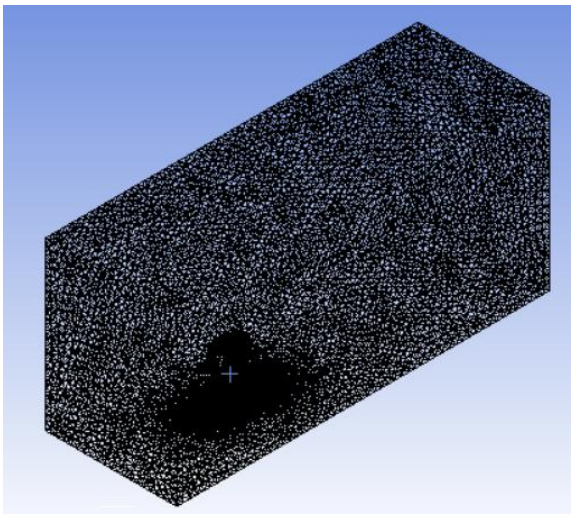

Figure 2. Three-dimensional domain of the cyclist on the dropped position with a standard helmet.

During a race, the mean speed is about 11.1 m/s (~ 40 km/h) [17]. The velocity was set at the inlet portion of the enclosure surface (-z direction) at 11.1 m/s (~ 40 km/h). The turbulence intensity was assumed as $1 \times 10^{-6\%}$. The bicycle-cyclist system surface was established as zero roughness, non-slip wall and scalable wall functions were assigned.

2.4. Numerical simulations

The Fluent CFD code (Ansys Fluent 16.0, Ansys Inc., Pennsylvania, USA) run the Reynolds-averaged Navier–Stokes (RANS) equations (equations 5, 6, 7 and 8) and assess the fluid flow behavior (equation 5), Reynolds Stresses (equation 6), temperature (equation 7) and mass transfer (equation 8). The RANS equations transform instantaneous values into means. Fluent CFD code (Ansys Fluent 16.0, Ansys Inc., Pennsylvania, USA) solve these equations by the finite volume approach. The Realizable k-e was selected as the turbulence model where the velocity histograms are very similar to the standard k-e, RST and RNG k-e models [18]. The standard wall function was selected for this simulation.

$$\frac{\partial U_i}{\partial x_i} = 0 \tag{5}$$

$$\frac{\partial U_i}{\partial_t} \pm U_j \frac{\partial U_i}{\partial x_j} = -\frac{1}{\rho}\frac{\partial P}{\partial x_j} + \frac{\partial}{\partial x_j}\left(2vS_{ij} - \overline{\mu_j{}'\mu_\iota{}'}\right) \tag{6}$$

$$\frac{\partial \theta_i}{\partial_t} \pm U_j \frac{\partial \theta}{\partial x_j} = \frac{1}{\rho c_p}\frac{\partial}{\partial x_j}\left(k\frac{\partial \theta}{\partial x_j} - \overline{\mu_j{}'\theta'}\right) \tag{7}$$

$$\frac{\partial C}{\partial t} \pm U_j \frac{\partial C}{\partial x_j} = \frac{\partial}{\partial x_j}\left(D\frac{\partial C}{\partial x_j} - \overline{\mu_j{}'c'}\right) \tag{8}$$

Where, U_i and x_i are the instantaneous velocity and the position, p the instantaneous pressure, t is the time, ρ the fluid density, v is the molecular kinematic viscosity, c_p heat capacity, k is the thermal conductivity and S_{ij} the strain-rate tensor, c is the instantaneous concentration, and D is the molecular diffusion coefficient. The Reynolds stresses component ($\overline{\mu_j{}'\mu_\iota{}'}$), describes the turbulence of the mean flow being the exchange of momentum by the change of the fluid parcels. The Reynolds stress is given by:

$$\overline{\mu_j{}'\mu_\iota{}'} = 2v_t S_{ij} - \frac{2}{3}TKE\delta_{ij} \tag{9}$$

Where, v_t is the turbulent viscosity and the mean strain rate S_{ij} is given by,

$$S_{ij} = \frac{1}{2}\left(\frac{\partial U_i}{\partial_{xj}} + \frac{\partial j}{\partial_{xi}}\right) \tag{10}$$

The turbulent kinetic energy (*TKE*) is given by,

$$TKE = \frac{1}{2}\overline{\mu_\iota{}'\mu_\iota{}'} \tag{11}$$

And the kronecker delta (δ_{ij}),

$$\delta_{ij} = \begin{cases} 1;\ if\ i = j \\ 0; if\ i \neq j \end{cases} \tag{12}$$

The SIMPLE algorithm was used for pressure–velocity coupling. The pressure interpolation and the convection and viscous terms of the governing equations discretization schemes were defined as second. The least-squares cell-based method computed the gradients. Pressure and momentum were defined as second order and second order upwind and the turbulent kinetic energy and turbulent dissipation rate as first order upwind. The convergence occurred automatically by the Ansys Fluent 16.0 (Ansys Fluent 16.0, Ansys Inc., Pennsylvania, USA) before 1,404 interactions.

2.5. Outcomes

After the numerical simulations, outputs such as viscous, pressure, total drag and coefficient of

drag are possible to obtain. Ansys Fluent Software (Ansys Fluent 16.0, Ansys Inc., Pennsylvania, USA) computed the surface area.

To compute the drag force, equation (13) was used:

$$F_d = \frac{1}{2}\rho A C_d v^2 \tag{13}$$

Where, F_d is the drag force, C_d represents the drag coefficient, v the velocity, A the surface area and ρ is the air density (1.292 kg/m^3).

Pressure coefficient (Cp) and relative velocity magnitude (m/s) graphical representation were obtained in Ansys Fluent 16.0 (Ansys Fluent 16.0, Ansys Inc., Pennsylvania, USA) after the numerical simulations. The contours of pressure and velocity were obtained without filled geometries.

3. Results

The aero road helmet presented a lower viscous, pressure and total drag in comparison to the standard helmet (Figure 3). The standard helmet presented a viscous drag of 10.52 N and the aero road helmet 7.40 N. The pressure drag of the standard helmet was 16.51 N for the selected speed and 12.56 N for the aero road helmet. Moreover, the total drag of the standard helmet was 21.98 N and the aero road helmet was 19.96 N.

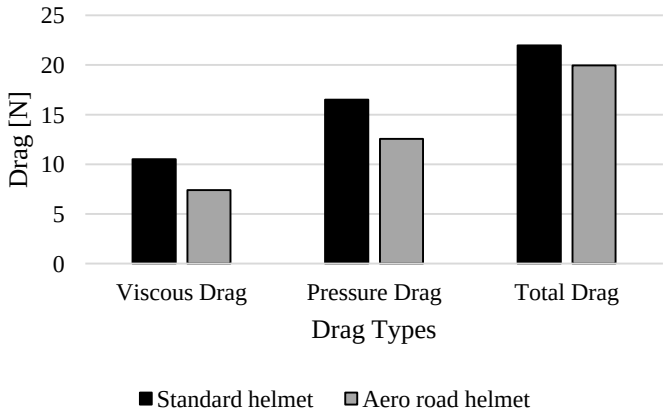

Figure 3. Viscous, pressure and total drag at 11.11 m/s for the standard and aero helmet.

The aero road helmet presented a lower viscous, pressure and total drag coefficient in comparison to the standard helmet (Figure 4). The standard helmet presented a viscous drag coefficient of 0.30 and the aero road helmet 0.21. The standard helmet pressure drag coefficient was 0.46 N for the selected speed and 0.35 for the aero road helmet. The total drag coefficient of the standard helmet was 0.76 and the aero road helmet was 0.56.

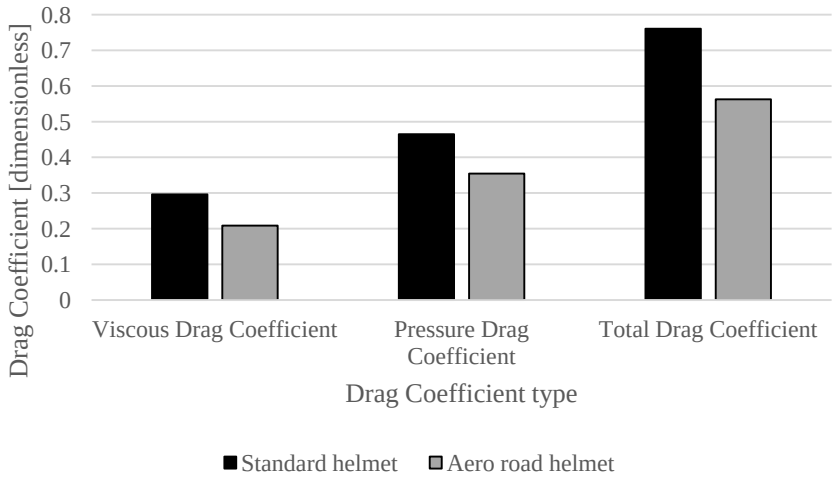

Figure 4. Viscous, pressure and total drag coefficient at 11.11 m/s for the standard and aero helmet.

The aero road helmet a lower pressure coefficient (Cp) in comparison to the standard helmet (Figure 5). The standard helmet presented a Cp between -3.94 and 1.08; whereas the aero road helmet presented a Cp between -3.63 and 1.05.

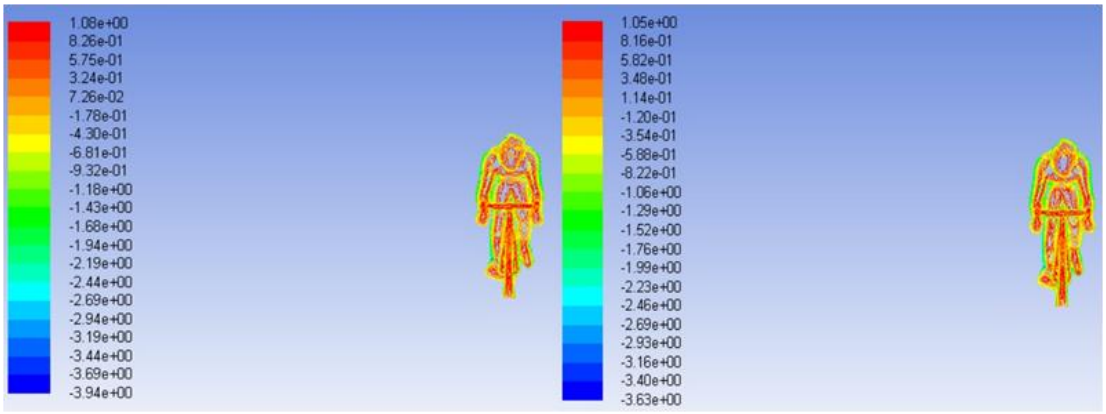

Figure 5. Coefficient of Pressure for standard helmet (left) and aero road helmet (right) at 11.11 m/s.

The aero road helmet presented a lower relative velocity magnitude (m/s) in comparison to the standard helmet (Figure 6). The relative velocity magnitude for the standard helmet ranged between 3.11×10^{-3} and 22.24 m/s. The relative velocity magnitude for the aero road helmet ranged between 2.87×10^{-3} and 22.2 m/s.

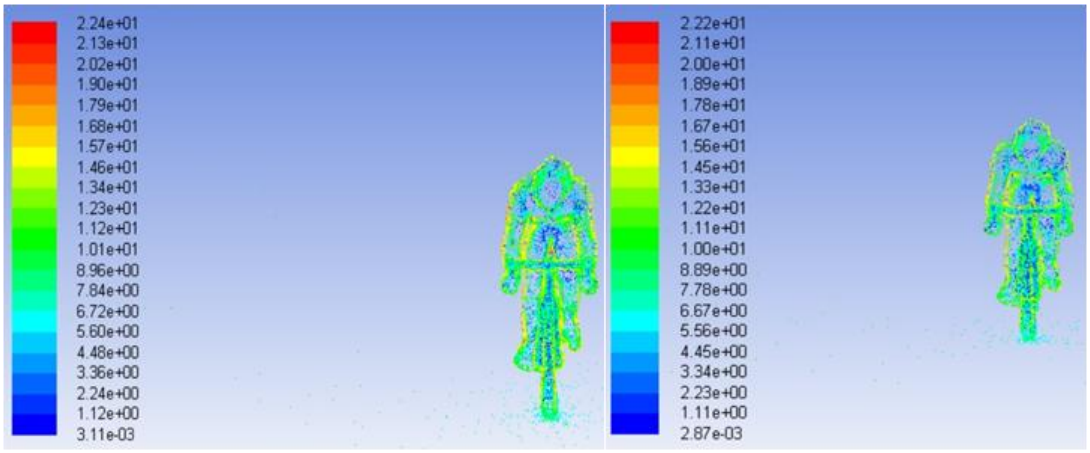

Figure 6. Relative velocity magnitude in (m/s) for standard helmet (left) and aero road helmet (right) at 11.11 m/s.

4. Discussions

The aim of this study was to assess the aerodynamics of an elite cyclist wearing a standard and an aero road helmet on the dropped position by computer fluid dynamics. The main results were that the aero road helmet presented lower viscous, pressure and total drag, such as viscous, pressure and total drag coefficient.

An elite level cyclist volunteered for this research. Aerodynamic analysis by CFD are usually made with elite subjects, representatives of the sport [3,4,13]. Cyclist's averaged speed in tours is near 11.11 m/s (≈ 40 km/h) [17]. This was the selected speed to assess drag in our study. Moreover, during a race, the dropped position is one of the adopted positions to minimize drag in comparison to the normal position [7]. In our study, the dropped position was the selected position. The numerical simulations by CFD has been used to assess cyclists drag in different situations [12,13]. CFD presented concordance with wind tunnel experiments [7,19,20].

The standard helmet imposed a higher drag in comparison to the aero road helmet. The standard helmet total was 21.98 N and the aero road helmet 19.96 N. Forte et al. [21], compared a standard and an aero helmet at wheelchair racing speeds (maximal 6.5 m/s). The differences between helmets were near 30%. However, the authors only evaluated the head and helmet. In our study, the bicycle-cyclist system was assessed with the different helmets and the total drag differences was 9%. The differences magnitude might be explained by: (i) the selected speeds were different; (ii) the fluid flow around the bicycle-cyclist geometry was different from the head and helmet. Brownlie et al. [22], also reported that time trial helmets reduce the cyclists drag. These findings seem to be in accordance with our study. The drag coefficient with the standard helmet was 0.76 and the aero road helmet was 0.56. The drag coefficient is dependent of the geometry form or shape [23,24]. Moreover, the fluid flow between helmets may also explain the drag coefficient changes [23–25]. In our study, the difference between the two helmets in drag coefficient was 26%. In Beaumont et al. [3] study, the drag coefficient differences between three helmets were about 3.1%. However, the authors only assessed drag with the cyclist body and the bicycle was not included in the analysis. In our study, the pressure coefficient was slightly higher in the standard helmet in comparison to the aero road helmet. The same phenomenon was observed in the relative velocity magnitude between helmets. The reduced air

vents might also explain the differences between the helmets. Helmets with smooth surfaces are designed by engineers and sports scientists to minimize drag coefficient [3,14,15]. This may also contribute to reduce parasite turbulence and drag [26].

Overall, the pressure coefficient and relative velocity magnitude did not presented an accentuated difference. This is supported by the Blocken et al. study [7], the authors reported Cp near -1 and 1. In our study, the highest Cp was 1.08. This may suggest that the drag differences were due the fluid flow around bicycle-cyclist geometries with the different helmets [21, 23–26]. In our study, the selected aero road helmet presented less air vents and drag coefficient in comparison to the standard type. Upon that, cycling practitioners may choose to use aero road helmets type with reduce air vents to produce the wind-cheating effects of time-trial helmets instead of normal helmets with front/side and back air channels.

The present study present the following limitations: (i) only one position was assessed; (ii) the cyclist spent more time in the normal position than in the dropped position; (iii) numerical simulations were only performed at one speed; (iv) different temperatures were not tested; (v) the cyclist was only representative of elite level, so results might not be extrapolated to others. It can be addressed as further research: (i) comparisons between more helmets types; (ii) design and customize a specific helmet for the athlete; (iii) assess drag with different temperatures and positions; (iv) evaluate active drag by numerical simulations.

5. Conclusions

It is possible to conclude that an aero road helmet imposes less drag in comparison to a standard helmet. Thus, coaches should advise their athletes to use aero road helmets during a race. The resistance acting on an elite cyclist in the dropped position was higher with a standard helmet than with an aero road helmet.

Acknowledgments

This work is supported by national funding through the Portuguese Foundation for Science and Technology, I.P., under project UID/DTP/04045/2019.

Conflict of interest

All authors declare no conflicts of interest in this paper.

References

1. Barbosa TM, Forte P, Morais JE, et al. (2016) Analysis of the aerodynamics by experimental testing of an elite wheelchair sprinter. *11th conference of the International Sports Engineering Association, Elsevier,* 147: 2–6.
2. Barelle C, Chabroux V, Favier D (2010) Modeling of the time trial cyclist projected frontal area incorporating anthropometric, postural and helmet characteristics. *Sport Eng* 12: 199–206.
3. Beaumont F, Taiar R, Polidori G, et al. (2018) Aerodynamic study of time-trial helmets in cycling racing using CFD analysis. *J Biomech* 67: 1–8.

4. Defraeye T, Blocken B, Koninckx E, et al. (2010) Aerodynamic study of different cyclist positions: CFD analysis and full-scale wind-tunnel tests. *J Biomech* 43: 1262–1268.
5. Gross AC, Kyle CR, Malewicki DJ (1983) The aerodynamics of human-powered land vehicles. *Sci Am* 249: 142–153.
6. Kyle CR, Burke E (1984) Improving the racing bicycle. *Mech Eng* 106: 34–45.
7. Blocken B, van Druenen T, Toparlar Y, et al. (2018) Aerodynamic analysis of different cyclist hill descent positions. *J Wind Eng Ind Aerod* 181: 27–45.
8. Underwood L, Schumacher J, Burette-Pommay J, et al. (2011) Aerodynamic drag and biomechanical power of a track cyclist as a function of shoulder and torso angles. *Sport Eng* 14: 147–154.
9. Kyle CR (1996) Selecting cycling equipment, In: Burke, E.R., *High-tech cycling*, 2 Eds., Champaign, Illinois: Human Kinetics, 1–48.
10. Burke ER, Pruitt AL (2003) Body positioning for cycling. In: Burke, E.R., *High-tech cycling*, 2 Eds., Champaign, Illinois: Human Kinetics, 69–92.
11. Fintelman DM, Sterling M, Hemida H, et al. (2014) Optimal cycling time trial position models: Aerodynamics versus power output and metabolic energy. *J Biomech* 47: 1894–1898.
12. Forte P, Barbosa TM, Marinho DA (2015) Technologic appliance and performance concerns in wheelchair racing–helping Paralympic athletes to excel, In: Liu, C., *New Perspectives in Fluid Dynamics*, Rijeka, Croatia: IntechOpen, 101–121.
13. Forte P, Marinho DA, Morais JE, et al. (2018) The variations on the aerodynamics of a world-ranked wheelchair sprinter in the key-moments of the stroke cycle: A numerical simulation analysis. *PloS One* 13: e0193658.
14. Brühwiler PA, Buyan M, Huber R, et al. (2006) Heat transfer variations of bicycle helmets. *J Sport Sci* 24: 999–1011.
15. Forte P, Marinho DA, Morouço P, et al. (2017) Comparison by computer fluid dynamics of the drag force acting upon two helmets for wheelchair racers. *AIP Conference Proceedings*, AIP Publishing LLC, 1863: 520005.
16. Blocken B, Defraeye T, Koninckx E, et al. (2013) CFD simulations of the aerodynamic drag of two drafting cyclists. *Comput Fluids* 71: 435–445.
17. El Helou N, Berthelot G, Thibault V, et al. (2010) Tour de France, Giro, Vuelta, and classic European races show a unique progression of road cycling speed in the last 20 years. *J Sport Sci* 28: 789–796.
18. Aroussi A, Kucukgokoglan S, Pickering SJ, et al. (2001) Evaluation of four turbulence models in the interaction of multi burners swirling flows. *4th International Conference On Multiphase Flow*.
19. Blocken B, Toparlar Y (2015) A following car influences cyclist drag: CFD simulations and wind tunnel measurements. *J Wind Eng Ind Aerod* 145: 178–186.
20. Defraeye T, Blocken B, Koninckx E, et al. (2010) Aerodynamic study of different cyclist positions: CFD analysis and full-scale wind-tunnel tests. *J Biomech* 43: 1262–1268.
21. Forte P, Marinho DA, Morouço P, et al. (2017) Comparison by computer fluid dynamics of the drag force acting upon two helmets for wheelchair racers. *AIP Conference Proceedings*, AIP Publishing LLC, 1863: 520005.
22. Brownlie L, Ostafichuk P, Tews E, et al. (2010) The wind-averaged aerodynamic drag of competitive time trial cycling helmets. *Procedia Eng* 2: 2419C2424.

23. Pugh LGCE (1971) The influence of wind resistance in running and walking and the mechanical efficiency of work against horizontal or vertical forces. *J Physiol* 213: 255–276.
24. Debraux P, Grappe F, Manolova AV, et al. (2011) Aerodynamic drag in cycling: methods of assessment. *Sport Biomech* 10: 197–218.
25. Schlichting H, Gersten K (1979) Boundary-Layer Theory. MacGraw Hill, New York.
26. Abdullah MN, Muda MKH, Mustapha F, et al. (2017) Aerodynamics analysis for an outdoor road cycling helmet and air attack helmet. *Int J Mater Mech Manuf* 5: 46–50.

AIMS Press